

Comparison of CC Triple and Double Bonds as Spacers in Push–Pull Chromophores

Brian B. Frank,^[a] Philip R. Laporta,^[b] Benjamin Breiten,^[a] Mark C. Kuzyk,^[b] Peter D. Jarowski,^[a] W. Bernd Schweizer,^[a] Paul Seiler,^[a] Ivan Biaggio,^[b] Corinne Boudon,^[c] Jean-Paul Gisselbrecht,^[c] and François Diederich*^[a]

Keywords: Alkynes / Charge transfer / Conjugation / Donor–acceptor systems / Non-linear optics / Optoelectronic properties / Chromophores

We report the synthesis and properties of two series of homologous donor–acceptor (D–A) chromophores in which *N,N*-dimethylanilino (DMA) or *N,N*-dihexylanilino (DHA) donors and dicyanovinyl acceptors are separated by up to four C≡C triple-bond spacers or up to three C=C double-bond spacers. The intramolecular charge-transfer (CT) interactions of the new D–A oligoynes and the known all-*trans* D–A oligoynes were investigated by X-ray crystallography, electrochemistry, UV/Vis spectroscopy, and theoretical calcu-

lations. In both series, the optical and electrochemical HOMO–LUMO gaps decrease with increasing spacer length. The HOMO–LUMO gaps for the D–A oligoynes and oligoynes with a given spacer length are nearly identical. The effect of the spacer length was found to level-off for spacers with more than six carbon atoms. The third-order optical nonlinearity of both series of molecules was determined by measuring the rotational averages of the third-order polarizabilities γ_{rot} by degenerate four-wave mixing.

Introduction

Donor–acceptor (D–A) chromophores continue to attract considerable interest due to their electronic and optical properties, in particular, their second- and third-order optical nonlinearities.^[1] We have reported high third-order optical nonlinearities for four classes of small push–pull chromophores, linearly conjugated donor–acceptor-substituted tetraethynylethenes (TEEs),^[2] donor-substituted cyanoethynylethenes (CEEs),^[3] donor-substituted 1,1,4,4-tetracyanobuta-1,3-dienes (TCBDs),^[4,5] and recently also for homoconjugated systems.^[6] In addition, we have shown that one of the *N,N*-dimethylanilino (DMA)-substituted non-planar TCBDs (DDMEBT, {2-[4-(dimethylamino)phenyl]-3-[4-(dimethylamino)phenyl]ethynyl}buta-1,3-diene-1,1,4,4-tetracarbonitrile) forms high-optical-quality, homogeneous thin films by vapor-phase deposition.^[7] These films have found applications as materials in integrated nonlinear optics (NLO).^[8,9]

It has long been known that the off-resonant, that is, nonabsorptive, third-order polarizability strongly increases when the energy associated with the transition from the ground to the first excited state (HOMO–LUMO gap) decreases.^[10] Furthermore, it depends on the extension of the linear D–A conjugation pathways.^[11,12] Stronger D–A coupling across shorter π -conjugated spacers leads to higher-energy absorptions, whereas weaker D–A coupling across longer spacers results in lower HOMO–LUMO gaps.^[3b,4b,13–15] When the size of the spacer between the donor and acceptor groups is maintained constant,^[16] the HOMO–LUMO gap decreases with the π -conjugation efficiency. Some of these postulates were recently further validated in the investigation of the linear and third-order nonlinear optical properties of small push–pull chromophores bearing DMA donor and C(CN)₂ acceptor units.^[17,18] The best of these molecules have a third-order optical nonlinearity, represented by the rotational average of the third-order polarizability, γ_{rot} , which is very large relative to their size^[18] and approached the theoretically predicted fundamental limit.^[19]

Popular π -conjugated spacers connecting the D and A in push–pull chromophores comprise *trans*-substituted C=C double bonds, C≡C triple bonds, or mixed enyne systems. However, direct comparisons under identical experimental conditions of the efficiency of olefinic and acetylenic spacers in enhancing third-order optical nonlinearities of push–pull chromophores are rare.

Comparisons of the electrochemical and optoelectronic properties of C=C double and C≡C triple bond spacers

[a] Laboratorium für Organische Chemie, ETH-Hönggerberg, HCI, 8093 Zürich, Switzerland
Fax: +41-44-632-1109
E-mail: diederich@org.chem.ethz.ch

[b] Lehigh University, Department of Physics, 415 Lewis Lab, 16 Memorial Dr. East, Bethlehem, PA 18015, USA

[c] Laboratoire d'Electrochimie et de Chimie Physique du Corps Solide, Institute de Chimie-UMR 7177, CNRS, Université de Strasbourg,

4, rue Blaise Pascal, CS 90032, 67081 Strasbourg Cedex, France
Supporting information for this article is available on the WWW under <http://dx.doi.org/10.1002/ejoc.201100378>.

have been reported for D- π -D systems (π = π -conjugated spacer) and for systems in which electroneutral substituents are linked by oligoenes and -ynes.^[20–22] The electronic and nonlinear optical properties of D-A-substituted oligoenes and -ynes have been compared in theoretical studies.^[23,24] D-A-substituted allenes have also been included in one theoretical comparison.^[25]

In experimental studies, a wide variety of D-A-substituted oligoenes have been prepared to investigate their second-order NLO behavior.^[26–30] The second-order NLO properties of D-A oligoynes have also been reported.^[31–33] Tykwinski and co-workers studied the third-order NLO properties of triisopropylsilyl (TIPS) and phenyl end-capped oligoynes of various lengths.^[19b,34,35] Only a few limited studies have been published on the third-order NLO properties of D-A-substituted oligoenes.^[36]

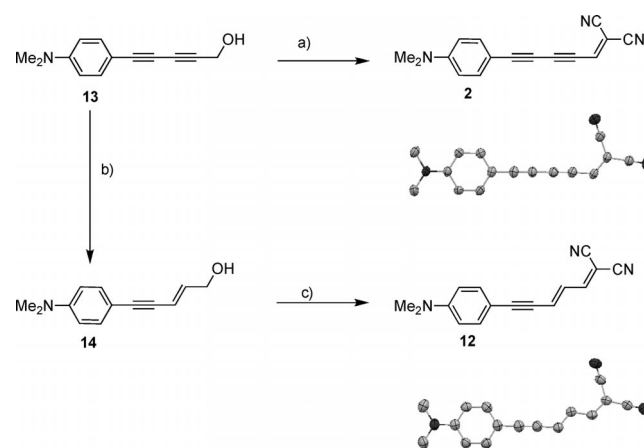
Herein we report a comparative investigation of the linear and third-order nonlinear optical properties of D-A oligoynes **1**^[4a] and **2–6** and oligoenes **7–11** (Figure 1) under identical conditions. The synthesis of pentayne **6** was also pursued but the compound was too unstable to isolate. Oligoenes **7** and **11** were only considered in the computational section of this work. The investigation also included compound **12** with a mixed enyne spacer. Although the oligoynes are new compounds, the oligoenes have previously been extensively studied as second-order NLO chromophores by Marder^[37] and Kawasaki^[38] and their co-workers. Blanchard-Desce and co-workers reported the second- and third-order NLO properties of the *N,N*-dibutylanilino (DBA)-substituted analogues of oligoenes **7–11**.^[36,39] Blanchard-Desce et al. also investigated the third-order NLO properties of different anilino-substituted oligoene series, up to a tetraene spacer and bearing *N,N'*-diethyl-3-thiobarbituric acid and 3-(dicyanomethylidene)-2,3-dihydrobenzo[*b*]thiophene 1,1-dioxide acceptor moieties.^[40] However, the third-order polarizabilities were measured by using third-harmonic generation (THG) under increasingly resonant conditions for the longer molecules. Direct comparison with the literature data is generally rendered difficult by the fact that the optical nonlinearities are strongly solvent-dependent and also dependent on the method of measurement. All NLO data in this work were obtained by degenerate four-wave mixing (DFWM) at the off-resonant wavelength of 1.5 μm with CH_2Cl_2 used as the solvent throughout the entire investigation. The study was also of

interest for its experimental contribution to the ongoing debate about the efficiency of CC double and triple bonds in transmitting conjugative effects.^[41]

Results and Discussion

Synthesis and Structures of D-A Oligoynes

D-A-substituted diyne **2** was prepared from DMA-substituted 2,4-pentadiyn-1-ol **13**^[42] by oxidation to the corresponding aldehyde with Dess–Martin periodinane (DMP) followed by Knoevenagel condensation with malononitrile in a “one-pot” set-up (Scheme 1).^[17] It is a dark-red solid, which is stable up to its melting point at around 145 °C, and was characterized by X-ray analysis [for details, see the Supporting Information (SI)]. For the preparation of enyne **12**, diyne **13** was regioselectively reduced to enyne **14** with sodium bis(2-methoxyethoxy)aluminium hydride (Red-Al[®]).^[43] Only the *trans* double bond was formed under these conditions, as confirmed by X-ray analysis (Scheme 1). Enyne **12** was subsequently obtained as a red solid by the “one-pot” oxidation/Knoevenagel condensation and is stable up to its melting point at 119–121 °C. ¹H NMR spectroscopy showed partial isomerization of the *trans* double bond to the *cis* double bond for CDCl_3 solutions of **12** on exposure to light. No isomerization was observed when CDCl_3 or CH_2Cl_2 solutions of **12** were kept in the dark. As a solid, **12** is photochemically stable. Thus, enyne **12** was synthesized, purified, and characterized in the absence of light.



Scheme 1. Synthesis and ORTEP plots of chromophores **2** and **12**. Reagents and conditions: a) 1. Dess–Martin periodinane (DMP), CH_2Cl_2 , 1.5 h, 25 °C; 2. $\text{CH}_2(\text{CN})_2$, Al_2O_3 , CH_2Cl_2 , 1 h, 50 °C, 47%; b) Red-Al[®], THF, 4 h, 0–25 °C, 52%; c) 1. DMP, CH_2Cl_2 , 1 h, 25 °C; 2. $\text{CH}_2(\text{CN})_2$, Al_2O_3 , CH_2Cl_2 , 6 h, 50 °C, 38%. For further details of the crystal structures, see the SI.

The synthesis of **3** and **4** started with the oxidative Hay heterocoupling of diynes **15**^[4b] and **16**^[44] with an excess of prop-2-yn-1-ol to give triynes **17** and **18**, respectively (Scheme 2), which were transformed, as described above, into **3** and **4**. The DHA substituent in **4** enhances its solubility, whereas DMA-substituted **3** exhibits poor solubility in common organic solvents (e.g., CHCl_3 or CH_2Cl_2).

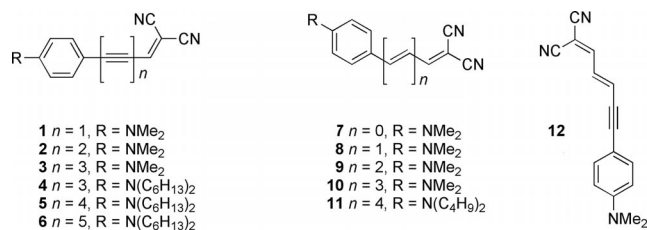
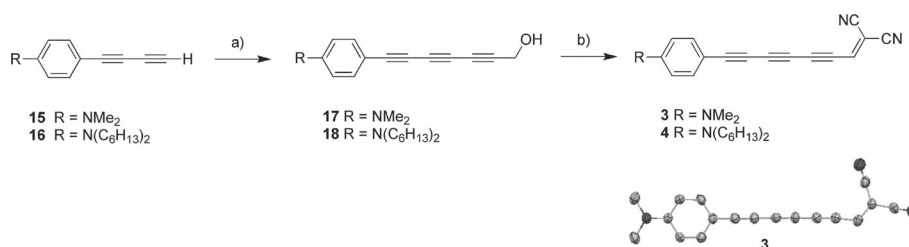


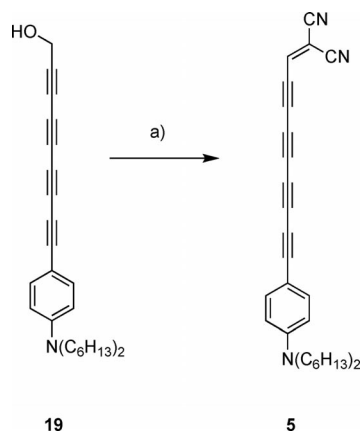
Figure 1. D-A-substituted oligoynes **1–6**, oligoenes **7–11**, and enyne **12**.



Scheme 2. Synthesis of the D–A triynes **3** and **4** and ORTEP plot of chromophore **3**. Reagents and conditions: a) prop-2-yn-1-ol (4 and 15 equiv. for **17** and **18**, respectively), CuCl, *N,N,N',N'*-tetramethylethylenediamine (TMEDA), CH₂Cl₂, 25 °C, 53% (**17**), 68% (**18**); b) 1. DMP, CH₂Cl₂, 1 h, 25 °C; 2. CH₂(CN)₂, Al₂O₃, CH₂Cl₂, 1 h, 50 °C, 48% (**3**), 19% (**4**). For details of the crystal structure, see the SI.

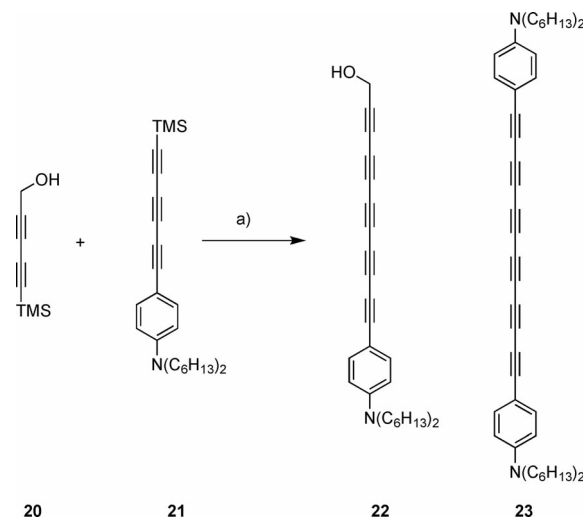
Dark-blue **4** was stable when subjected to severe agitation and was characterized by X-ray analysis (Scheme 2). However, explosive decomposition was observed at temperatures over 180 °C. Triyne **4** seems to be stable up to its melting point at around 65 °C.

The D–A-substituted tetrayne **5** was prepared from alcohol **19**^[45] by the “one-pot” oxidation/Knoevenagel condensation method (Scheme 3). Similarly to its precursor, **5** exhibits very low thermal stability: Decomposition was observed at 40 °C during evaporation of the solvent. Thus, the Knoevenagel condensation with malononitrile was performed at 25 °C. DMP oxidation of **19** was completed after 10 min.



Scheme 3. Synthesis of D–A-substituted tetrayne **5**. Reagents and conditions: a) 1. DMP, CH₂Cl₂, 10 min, 25 °C; 2. CH₂(CN)₂, Al₂O₃, CH₂Cl₂, 1 h, 25 °C, 38%.

For the synthesis of D–A-substituted pentayne **6**, compounds **20**^[46] and **21**,^[45] upon deprotection of the TMS group, were subjected to oxidative Hay heterocoupling to afford **22** together with the symmetric hexayne **23** (Scheme 4).^[45] Pentayne **22** was handled and stored at temperatures below 40 °C because of its low thermal stability. The synthesis of **6** was attempted by the “one-pot” oxidation/Knoevenagel condensation method. However, the target compound could not be obtained in pure form due to its low thermal stability.



Scheme 4. Synthesis of pentayne **22** and hexayne **23**.^[45] Reagents and conditions: a) 1. K₂CO₃, MeOH/THF (1:1), 2 h, 25 °C; 2. TMEDA, MeOH/THF/CH₂Cl₂ (1:1:1), 16 h, 25 °C, 23% (**22**), 24% (**23**).

The known D–A oligoenes **8–10** were synthesized according to literature procedures.^[37,38] The three chromophores are thermally and photochemically stable as solids over periods of months. However, CDCl₃ and CH₂Cl₂ solutions show partial isomerization after exposure to light for 24 h (see Figures S1 and S2). To prevent the photochemical *trans/cis* isomerization of the double bonds of the oligoene chromophores and their precursors, they were synthesized, purified, and characterized in the absence of light.

Electrochemistry

The electrochemical investigations of the new D–A oligoynes and the known D–A oligoenes were carried out by cyclic voltammetry (CV) and rotating disk voltammetry (RDV) in CH₂Cl₂ with *n*Bu₄NPF₆ (0.1 M) as the supporting electrolyte. The redox potentials versus Fc⁺/Fc (ferrocinium/ferrocene couple) for the D–A oligoynes and oligoenes are listed in Table 1. Comparisons of the redox properties of the oligoynes and -enes have previously been reported and are further discussed in the SI.^[20–22] For systems with the

general structure D- π -D, the first reduction potentials of the oligoynes are anodically shifted relative to oligoenes containing the same number of unsaturated CC bonds.^[20–22,47] The data reported below also validate these trends for D- π -A systems. Also, the redox properties recorded for oligoenes **8–10** are in good agreement with those reported by Marder and co-workers for **8** and **9**,^[48] and by Blanchard-Desce and co-workers for the corresponding DBA derivatives of **8–10**.^[36]

Table 1. Cyclic voltammetry (CV; scan rate $\nu = 0.1 \text{ V s}^{-1}$) and rotating disk voltammetry (RDV) data in CH_2Cl_2 (+0.1 *m* $n\text{Bu}_4\text{NPF}_6$).^[a]

	CV			RDV	
	E° [V] ^[b]	ΔE_p [mV] ^[c]	E_p [V] ^[d]	$E_{1/2}$ [V] ^[e]	Slope [mV] ^[f]
1 ^[g]	+0.66 ^[h]			+0.70 (1e ⁻)	70
2	+0.62	100	-1.50	-1.50 (1e ⁻)	100
3	+0.59	100	-1.33	+0.63 (1e ⁻)	65
4	+0.58	60	-1.02	-1.24 (1e ⁻)	75
5	+0.55	80	-1.07	+0.55	60
8	+0.53	100	-1.09	-1.07	75
9	+0.36	100	-1.07	+0.59	60
10	+0.25	75	-1.07	-1.06	60
			-1.09	+0.56 (1e ⁻)	60
			-1.09	-1.09 (1e ⁻)	60
			-1.63	+0.54 (1e ⁻)	65
			-1.52	-1.66 (1e ⁻)	100
			-1.43	+0.36 (1e ⁻)	65
				-1.56 (1e ⁻)	220
				+0.25 (1e ⁻)	60
				-1.45 (1e ⁻)	120

[a] All potentials are given vs. the Fc^+/Fc couple used as internal standard. [b] $E^\circ = (E_{pc} + E_{pa})/2$ in which E_{pc} and E_{pa} correspond to the cathodic and anodic peak potentials, respectively. [c] $\Delta E_p = E_{pa} - E_{pc}$. [d] E_p is irreversible peak potential. [e] $E_{1/2}$ = half-wave potential. [f] Logarithmic analysis of the wave obtained by plotting E vs. $\log[I/(I_{lim} - I)]$. [g] See ref.^[4a] [h] Scan rate $\nu = 2.0 \text{ V s}^{-1}$.

All D-A-substituted oligoynes show an irreversible 1e⁻ reduction step occurring at the dicyanovinyl moiety. The first reduction potentials of triynes **3** [-1.07 V (RDV)] and **4** [-1.06 V (RDV)] in CV and RDV are nearly identical. When going from monoyne **1** to tetrayne **5**, the value of $E_{red,1}$ shifts anodically from -1.50 to -1.09 V in CV. Interestingly, the most anodically shifted reduction potentials in the entire series are found for triynes **3** [-1.02 V (CV)] and **4** [-1.07 V (CV)] and not for the longer tetrayne **5**. This indicates that the effect of the spacer length on the reduction potential of D-A oligoynes is negligible in compounds with more than three C \equiv C triple bonds (see below).

The first oxidation potentials in CV are cathodically shifted from +0.66 V in monoyne **1**^[4a] to +0.55 V in tetrayne **5** due to the reduced transfer of electron density from the donor to the acceptor with increasing spacer length. However, the potential shift for the oxidation process is less pronounced (ca. 100 mV difference) than for the reduction process (ca. 400 mV difference). The donor properties of the DMA and DHA moieties are quite similar, as seen in the comparison of the two triynes **3** and **4**.

In the series of oligoenes, the oxidation potentials are cathodically shifted when increasing the spacer length from monoene **8** (+0.53 V)^[48] to diene **9** (+0.36 V)^[48] and triene **10** (+0.25 V). The irreversible (CV) 1e⁻ reduction on the

dicyanovinyl moiety is also increasingly facilitated upon increasing the length of the spacer [**8** (-1.63 V), **9** (-1.52 V), and **10** (-1.43 V); a difference of ca. 200 mV], but not as much as in the corresponding oligoyne series (a difference of ca. 480 mV). Also, the potential shift of the oxidation process in the oligoene series is more pronounced (ca. 280 mV difference) than for the reduction process (ca. 200 mV difference).

The electrochemical HOMO-LUMO gap, determined from the RDV results, decreases along the oligoyne series from 2.20 V for **1** down to 1.62 V for **3** (see Table 2). Note that the values of the electrochemical HOMO-LUMO gaps are rather approximate due to the irreversible nature of the reduction steps in the series. However, these results clearly show that up to the D-A triyne there is less efficient coupling between the aniline donor and the dicyanovinyl acceptor with increasing spacer length.

In the oligoene series, the electrochemical HOMO-LUMO gap decreases from 2.20 (**8**) to 1.70 V (**10**, RDV). Interestingly, the electrochemical HOMO-LUMO gaps of D-A oligoynes and oligoenes are quite similar or even identical, as in the case of **1** and **8** [2.20 V (RDV)] even though their individual oxidation and reduction potentials differ considerably. The similarity between the HOMO-LUMO gaps in both series is also seen in the optical gaps, determined by UV/Vis spectroscopy (see below).

The enyne **12** exhibits an irreversible 1e⁻ oxidation of the aniline moiety at +0.56 V. This value is much closer to the potential recorded for tetrayne **5** (+0.55 V) than for diyne **2** (+0.62 V) and shows a strong influence of the spacer structure on the redox properties. Also, the first reduction potential is strongly cathodically shifted upon exchanging a CC triple bond in diyne **2** [$E_{red,1} = -1.24 \text{ V}$ (RDV)] to a CC double bond in enyne **12** [$E_{red,1} = -1.43 \text{ V}$ (RDV)].

UV/Vis Spectroscopy

Both D-A-substituted oligoyne and -ene chromophores feature one intramolecular CT band in their UV/Vis spectra recorded in CH_2Cl_2 . The longest wavelength maximum λ_{max} of the D-A oligoynes appears between 477 (2.60 eV, **1**^[4a]) and 573 nm (2.17 eV, **5**; Figure 2) and the intensity of the CT band drops with increasing spacer length from **1** ($\epsilon = 44100 \text{ M}^{-1} \text{ cm}^{-1}$) to **5** ($\epsilon = 10100 \text{ M}^{-1} \text{ cm}^{-1}$). The CT character of the longest-wavelength absorption was confirmed by protonation/neutralization experiments (see the SI). The spectra of oligoenes **8–10** are depicted in Figure S7 and are in good agreement with previously reported data.^[36,37,48] The electrochemical HOMO-LUMO gaps and the optical gaps determined either from the longest wavelength maxima or the end-absorption (λ_{end}) in the UV/Vis spectra are presented in Table 2. Plots of the optical gap against the electrochemical HOMO-LUMO gap in both series gave a strong linear correlation ($R^2 = 0.86$ for λ_{max} and $R^2 = 0.96$ for λ_{end}) between the two quantities (Figures S8 and S9), which indicates that the same HOMO and LUMO orbitals are involved.

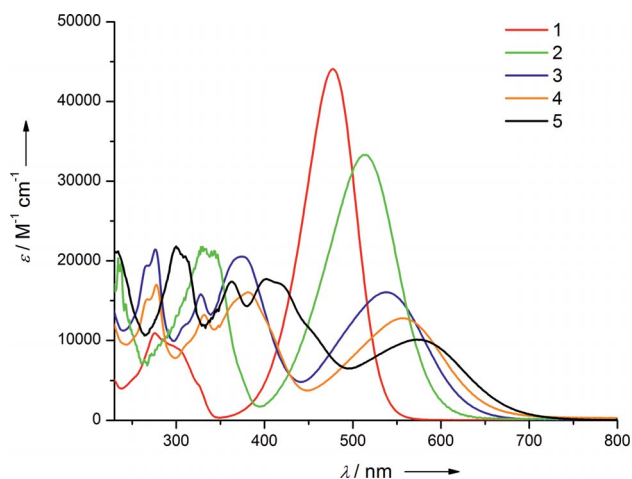


Figure 2. UV/Vis spectra of D–A oligoynes **1–5** in CH₂Cl₂ at 298 K.

Table 2. Optical and electrochemical gaps determined by UV/Vis spectroscopy and RDV in CH₂Cl₂ and computed values based on the TD-B2LYP/6-31G(d) method.

	Experimental				Computed	
	λ_{\max} [nm]	ϵ [M ⁻¹ cm ⁻¹]	λ_{end} [nm (eV)]	$\Delta(E_{\text{ox},1} - E_{\text{red},1})$ [V]	λ_{\max} [nm]	$f^{\text{[a]}}$
1 ^[b]	477	44100	590 (2.11)	2.20	416	1.0
2	512	33300	647 (1.92)	1.87	472	1.10
3	538	16100	782 (1.59)	1.62	529	1.08
4	560	12700	769 (1.62)	1.65		
5	573	10100	762 (1.63)	1.65	584 ^[c]	1.02
8	488	47000	590 (2.11)	2.20	408	1.20
9	519	35000	670 (1.85)	1.92	456	1.54
10	539	41700	793 (1.57)	1.70	502	1.84
12	505	35900	639 (1.94)	1.99		

[a] f = oscillator strength. [b] See ref.^[4a] [c] Calculated for the DMA-substituted derivative.

In line with the electrochemical data, the effect of the spacer on the optical gap slowly levels off on going from the triyne **3** ($\lambda_{\max} = 538$ nm) to the tetrayne **5** ($\lambda_{\max} = 573$ nm). Also, the optical gaps of the D–A oligoynes and -enes with spacers of equal length are quite similar.

Nonlinear Optical Properties

The rotational average of the third-order polarizability γ_{rot} of oligoynes **1–4**, oligoynes **8–10**, and enyne **12** were determined by measuring the third-order susceptibility $\chi^{(3)}_{1111}(-\omega, -\omega, \omega, \omega)$ of CH₂Cl₂ solutions of varying molecular concentration. The measurements were taken by degenerate four-wave mixing (DFWM) at 1.5 μm using 1 ps laser pulses obtained from a TOPAS travelling wave optical parametric amplifier system pumped by a Clark MXR amplified Ti:Sapphire laser. We used 1 mm thick solutions in fused silica spectroscopy cells, the concentrations of which were varied by successive dilutions and determined for each solution from the absorption spectrum calibrated to a reference spectrum of the molecular extinction coefficient. This guar-

antees an accurate determination of the molecular concentration that leads to the four-wave mixing signal even in those cases in which it was not possible to accurately control solvent evaporation and solute molecular mass for each dilution step, like for example when only limited quantities of a given compound were available and multiple filtration steps were needed when preparing the solution. In addition, comparison of the absorption spectrum of the solution used for the DFWM measurements with the reference spectrum was used to check the possibility of any decomposition, contamination, or isomerization during the NLO measurements.

For real-value third-order polarizability and low concentrations, the third-order susceptibility of the solution is proportional to the square root of the DFWM signal, which depends linearly on the concentration in units of mass per volume with a slope of $f^4 S^{-1/2} \gamma_{\text{rot}} \rho / m$ in which $f = (n^2 + 2)/3$ is a Lorentzian local field factor that depends on the refractive index $n = 1.4242$ of CH₂Cl₂, S is the DFWM signal of a cell containing only CH₂Cl₂, ρ is the mass density of CH₂Cl₂, and m is the mass of the molecule under investigation. We obtained absolute values for γ_{rot} by a reference measurement that established the DFWM signal S for a cell filled with pure CH₂Cl₂ to be 6 ± 1 times larger than for a 1 mm thick fused silica sample. For final calibration, we used a third-order susceptibility of $\chi^{(3)}_{1111}(-\omega, -\omega, \omega, \omega) = 1.9 \times 10^{-22}$ for fused silica at 1.5 μm .

Alkyne **1** has also been measured previously^[3a] but we have since discovered a calibration error for the experimental set-up used in refs.^[3a,4a,17,18] that caused the values of the third-order polarizabilities γ_{rot} reported there to be too large by a factor 1.5. The new value for **1** is in agreement with the value reported in ref.^[3a] divided by 1.5. Oligoynes **2** and **3** were increasingly difficult to dissolve, delivering solutions polluted by scattering particles that required multiple filtering steps, especially for **3**, which affected the accuracy of the DFWM measurements, which needed to be repeated multiple times. Molecule **4** delivered a better solution, but it could only be tested once because of the small quantity available. The problems observed with molecules **2** and **3** were greatly exacerbated for molecule **5**, which produced such a high level of scattering in solution that it made the DFWM measurements impossible. In addition, the spectrum of molecule **5** showed clear signs of decomposition, possibly originating from its intercontinental transfer, which led us to discard all nonlinear optical measurements for this molecule.

Diene-spaced **9** also showed some dissolution problems relative to both ethylene-linked **8** and triene-spaced **10** with the DFWM data from solutions of **9** generally having more noise. The absorption spectra of molecules **8–10** and **12** during and after the nonlinear optical measurements did not show any significant change though, from which we conclude that there was no change in the isomer distribution (all-*trans*) during the optical measurements.

The third-order NLO properties of the DBA analogues of DMA-substituted oligoynes **8–10** had previously been measured by Blanchard-Desce and co-workers.^[36] When re-

scaled to take into account an incorrect calibration,^[39] the values for the third-order polarizabilities γ_{rot} for the DBA analogues of **8–10** were 2.2×10^{-48} , 10×10^{-48} , and $43 \times 10^{-48} \text{ m}^5 \text{ V}^{-2}$, respectively. However, these values were obtained by third-harmonic generation (THG) from a wavelength of 1.9 μm , which means that the values for the longer molecule are three-photon resonant, which explains the steeper increase of third-order polarizability with length that is seen in that study^[36,39] compared with the present work in which the measurements are definitely more off-resonant by virtue of the DFWM measurements at 1.5 μm , which give a two-photon resonance at 750 nm instead of the three-photon resonance at 633 nm for the THG experiments. Overall, and considering also the different solvents that have been used, we are in remarkable agreement with the previous results^[36,39] published for the nonlinearities of the oligoynes **8–10**. Only diene-bridged **9** gave us some experimental difficulties that may have caused an underestimation of its third-order polarizability, but it is clear that the third-order polarizability for D–A oligoynes increases rapidly with the number of C=C moieties in the spacer. This is caused by a significant redshift of the longest-wavelength optical absorption accompanied by the increase in the size of the molecule.

Despite the initial tripling of the third-order polarizability on going from acetylene-spaced **1** to diyne-spaced **2**, there is no further comparable steep increase in the third-order polarizability with the number of spacers in the oligoynes. Molecule **3** shows a third-order polarizability that is only at the same level as **2**, and longer molecules do not show any measurable increase. Although the nonlinear optical results for the triple-bond molecules with longer spacers should not be considered very accurate because of the issues of solubility and decomposition mentioned above, from the behavior of the shorter molecules one could tenta-

tively say that triple bonds are less effective in generating high third-order optical nonlinearities in the studied series. Another observation is that although the HOMO–LUMO gap in the series of oligoynes decreases with the size of the spacer in a similar way to the oligoenes, the strength of the transition, as described by the molar extinction coefficient, decreases as the length of the molecules increases, whereas for the double-bond molecules the extinction coefficient remains approximately constant (see Figure S7). The smaller cross-section for the excitation of the larger oligoynes would then lead to a lesser enhancement of the third-order polarizability when compared with the oligoenes. However, a note of caution is necessary here because of the aforementioned stability problems that affect the nonlinear optical characterization of the oligoynes.

Note also that we previously determined the third-order polarizability of pentayne **24**^[45] (Table 3) to be quite large, proving that triple bond spacers can be very effective in creating a large nonlinearity, in contrast to what we see here for molecules **1–5**.

Table 3 also lists two other quantities that are useful for judging the nonlinear optical properties of a molecule. The first is a simple figure of merit, the specific third-order polarizability $\tilde{\gamma}$, obtained by dividing the experimental value for the third-order polarizability γ_{rot} by the molecular mass: It determines the potential bulk third-order susceptibility of a dense supramolecular assembly of molecules. The second is the intrinsic third-order polarizability γ_1 . The concept of intrinsic hyperpolarizability has been proposed as a scale-invariant measure of a molecule's nonlinear optical properties.^[49] For our third-order molecules, we define it as the ratio between the experimental rotational average of the third-order polarizability γ_{rot} and the corresponding fundamental limit in the centrosymmetric case, γ_{k} ,^[19a] which is also listed in Table 3.

Table 3. Summary of the NLO relevant characteristics of the molecules investigated in this study.^[a]

	M_{mol} [g mol ⁻¹]	N_{π}	n	Type	λ_{max} [nm]	ϵ [10 ³ M ⁻¹ cm ⁻¹]	γ_{rot} [10 ⁻⁴⁸ m ⁵ V ⁻²]	$\tilde{\gamma}$ [10 ⁻²³ m ⁵ V ⁻² kg ⁻¹]	γ_1 [$\gamma_{\text{rot}}/\gamma_{\text{k}}$]	γ_{k} [10 ⁻⁴⁸ m ⁵ V ⁻²]
1	221.26	14	1	T	477	44.1	3 ± 1	0.82	0.017	174
2	245.28	16	2	T	512	33.3	10 ± 3	2.46	0.031	323
3	269.30	18	3	T	538	16.1	9 ± 5	2.01	0.017	524
4	409.57	18	3	T	560	12.7	7 ± 3	1.03	0.011	623
5	433.59	20	4	T	573	10.1	–	–	–	886
24 ^[b]	625.30	24	5	T	624	15.1	60 ± 20	5.78	0.031	1954
12	247.29	16	2	D + T	505	35.9	5 ± 1.5	1.22	0.017	290
8	218.80	14	1	D	488	47.0	3.5 ± 1.5	0.96	0.018	195
9	264.27	16	2	D	519	35.0	6 ± 1	1.37	0.017	346
10	275.35	18	3	D	539	41.7	20 ± 2	4.37	0.038	529



[a] For each molecule, we give the molecular mass M_{mol} , the number of conjugated electrons N_{π} , the number of CC spacers n , the type of spacers (T = triple bond, D = double bond), the longest wavelength absorption maximum λ_{max} and the corresponding molar extinction coefficient ϵ , the experimental value of the third-order polarizability γ_{rot} (rotational average), the specific third-order polarizability $\tilde{\gamma}$ derived from it, and the intrinsic third-order susceptibility γ_1 defined in terms of the fundamental limit for centrosymmetric molecules, γ_{k} . [b] See ref.^[45]

We see that pentayne **24**^[45] is a very efficient molecule, with its intrinsic third-order polarizability almost reaching the largest value we observed (10) for the oligoenes and the high value of oligoyne **2**. Thus, the triple-bond spacers are potentially very effective, at least in the case of this molecule, which is more stable than oligoynes **3–5** and also has a different and stronger acceptor system.

Computational Studies

The molecular structures of the D–A oligoyne and -ene series were optimized at the B3LYP/6-31G(d) level of theory by using the software package Gaussian 03 (Figure S10).^[50] For **5**, the DMA moiety was used instead of the DHA moiety. All structures are confirmed ground-state minima according to the analysis of their analytical frequencies computed at the same level, which show no imaginary frequencies. Time-dependent density functional theory single-point calculations [TD B3LYP/6-31G(d)] were performed on these minima. The predicted transition energies (λ_{max}) and oscillator strengths (f) are given in Table 2. These transitions are composed mostly of HOMO-to-LUMO excitations and thus can best be described as intramolecular charge-transfer processes involving the transfer of electron density from the DMA donor to the dicyanovinyl acceptor, as depicted in the molecular orbital representations of these levels (Figure S10).

The calculated transition energies tend to be higher than the experimental data for both the oligoene and -yne series. However, the calculated values are in line with the expected accuracy of intramolecular charge-transfer (ICT) systems using this methodology, which can have an error up to and beyond ± 1 eV^[51] (for the complete set of compounds, there is a mean absolute deviation of 0.24 eV). Given that ICT systems are comparatively difficult to calculate accurately, the results here are quite good.^[52] In contrast, the calculated oscillator strengths do not agree qualitatively with the experimental results. Discrepancies occur for compound **1**, which has a lower calculated oscillator strength than compound **2**, whereas in the oligoene series, compound **9** has a larger value than **8**. The accuracy of the treatment of oscillator strength (f) is more difficult to assess, as quality experimental data is lacking.^[51] However, the TD B3LYP method has been benchmarked against various ab initio methods for the calculation of oscillator strengths and performs similarly to DFT/MRCI.^[53] Thus, the calculated data are of the highest quality reasonably attainable for treatment of the largest systems in these series. Suffice it to say, there is clearly an issue in the calculation of oscillator strength for the oligoene and -yne series in going from one CC multiple bond ($n = 1$) to two ($n = 2$) in which the former tends to be underestimated compared with the latter. Beyond this kink in the data, the predicted values are in qualitative agreement with the experimental results.

Conclusions

A series of homologous D–A oligoynes have been prepared in which DMA or DHA donors and dicyanovinyl

acceptors are separated by up to four C≡C triple bonds as spacers. The DMA-substituted mono-, di-, and triynes are thermally stable up to their melting points, whereas the tetrayne decomposes above 40 °C. Explosive decomposition at 180 °C was observed in the case of the DMA-triyne. The D–A pentayne could not be obtained due to its low thermal stability. The corresponding all-*trans* D–A oligoenes were synthesized following known procedures. These compounds, as well as enyne **12**, exhibit good thermal stability, but are sensitive to light, especially in solution. Partial photochemical *trans/cis* isomerization after 24 h of light exposure was observed by ¹H NMR spectroscopy for all the oligoenes. Therefore, they were synthesized, purified, and characterized in the absence of light or under reduced illumination. The all-*trans* configuration was confirmed by X-ray crystallographic analysis and NMR spectroscopy. X-ray crystallographic analysis revealed that the oligoyne and enyne chromophores are nearly fully planar in the solid state. The UV/Vis spectra of the highly colored chromophores feature intense intramolecular charge-transfer bands that shift bathochromically with increasing spacer length. Cyclic voltammetry and rotating disk voltammetry showed 1 e[−] oxidations centered on the DMA or DHA moieties and 1 e[−] reductions on the dicyanovinyl moieties. In both series, the electrochemical HOMO–LUMO gap decreases from 2.2 V for both monoene and -yne to values between 1.62 (triyne) and 1.70 V (triene). Thus, the optical and electrochemical gaps of D–A oligoynes and -enes with a given spacer length are almost identical. In the oligoyne series, the electrochemical gap is mainly influenced by the change in the reduction potentials, whereas the shift in the oxidation potentials is more pronounced for the oligoenes. The effect of spacer length levels off, that is, reaches saturation beyond six carbon atoms in both series.

The conclusions from the analysis of CC triple- and double-bond spacers with respect to enhancement of third-order optical nonlinearities are ambivalent: The oligoenes have a better ability to produce good homogeneous solutions for the nonlinear optical measurements and show a clear increase in third-order polarizability with the size of the spacer. This is not the case for the oligoynes studied here; the oligoynes were also much less capable of producing a good homogeneous solution with signs of decomposition for the larger molecules and the third-order polarizability was already saturated at the diyne. This instability prevented an extension of the chromophoric series to longer spacer lengths. On the other hand, pentayne **24** with a five-triple bond spacer and a much stronger acceptor moiety did show a very strong third-order nonlinearity. This result hints at a strong NLO potential for the acetylene spacers in suitably designed chromophores.

Experimental Section

Materials and General Methods: Reagents and solvents were purchased as reagent grade from Acros, ABCR, Aldrich, and Fluka and used as received. THF was freshly distilled from Na/benzophenone, toluene from Na, and CH₂Cl₂ from CaH₂ under N₂. For

all aqueous solutions, deionized water was used. The Hay catalyst refers to a freshly prepared solution of CuCl (65 mg, 0.66 mmol) and *N,N,N',N'*-tetramethylethylenediamine (TMEDA; 80 mg, 0.69 mmol) in CH₂Cl₂ (5 mL). All reactions, except Hay couplings, were performed under an inert atmosphere by applying a positive pressure of argon. Drying was performed in vacuo at 10⁻² Torr. Solvents for flash chromatography (FC), medium-pressure liquid chromatography (MPLC), plug filtrations, and extractions were of technical quality and distilled before use. The chromatographic separations were carried out on SiO₂ 60 (particle size 0.040–0.063 mm, 230–400 mesh; Silicycle). FC was carried out at an overpressure of 0.1–0.6 bar. Thin-layer chromatography (TLC) was conducted on SiO₂-layered glass plates (60 F₂₅₄, Merck) and visualization was performed with UV light (254 or 366 nm). Compounds **8**,^[37,38] **9**,^[37] **10**,^[37] **13**,^[42] **15**,^[4b] **16**,^[44] **19**,^[45] **20**,^[46] and **21**^[45] were prepared according to literature procedures.

Melting points were measured with a Büchi B-540 melting-point apparatus in open capillaries. Decomp. refers to decomposition. ¹H and ¹³C NMR spectra were measured with Varian Mercury 300, Bruker ARX 300, Bruker DRX400, Bruker AV400, or Bruker DRX 500 instruments at 298 K unless otherwise stated. Chemical shifts are reported in ppm relative to the signal of tetramethylsilane. Residual solvent signals in the ¹H and ¹³C NMR spectra were used as internal references. Coupling constants (*J*) are given in Hz. The apparent resonance multiplicity is described as s (singlet), br. s (broad singlet), d (doublet), dd (doublet of doublets), dt (doublet of triplets), t (triplet), q (quartet), sept. (septet), and m (multiplet). Infrared spectra (IR) were recorded neat with a Varian 800 FT-IR instrument. Absorption bands are reported in cm⁻¹. UV/Vis spectra were recorded with a Varian Cary-5 spectrophotometer. The spectra were recorded in CH₂Cl₂ in a quartz cuvette (1 cm) at 298 K. The absorption wavelengths are reported in nm with the extinction coefficient ϵ , given in M⁻¹cm⁻¹, in parentheses; shoulders are indicated as sh. High-resolution (HR) EI-MS spectra were recorded with a Waters Micromass AutoSpec-Ultima spectrometer, HR-ESI-TOF-MS spectra with a Bruker maXis ESI-Q-TOF spectrometer, and HR-FT-ICR-MALDI-MS and ESI-MS spectra with a Varian IonSpec Fourier Transform (FT) ICR instrument with 3-hydroxypyridine-2-carboxylic acid (3-HPA) or {(2*E*)-3-[4-(*tert*-butyl)phenyl]-2-methylprop-2-enylidene}malononitrile (DCTB) as matrix. The most important signals are reported in *m/z* units with M⁺ representing the molecular ion. The names of compounds were generated with ACD Name 9 by Advanced Chemistry Development Inc.

Electrochemistry: Electrochemical measurements were carried out at 20 °C in CH₂Cl₂ containing 0.1 M *n*Bu₄NPF₆ in a classic three-electrode cell. CH₂Cl₂ was purchased in spectroscopic grade from Merck, dried with molecular sieves (4 Å), and stored under Ar prior to use. Electrochemical grade *n*Bu₄NPF₆ was purchased from Fluka and used as received. The working electrode was a glassy carbon disk electrode (3 mm in diameter) used either motionless in cyclic voltammetry (CV; 0.1–10 V s⁻¹) or as a rotating-disk electrode in rotating disk voltammetry (RDV). The auxiliary electrode was a Pt wire and the reference electrode was either an aqueous Ag/AgCl electrode or a platinum wire used as a pseudo-reference electrode. All potentials are referenced to the ferricinium/ferrocene (Fc⁺/Fc) couple, used as an internal standard, and are uncorrected from ohmic drop. The cell was connected to an Autolab PGSTAT30 potentiostat (Eco Chemie BV, Utrecht, The Netherlands) driven by GPSE software running on a personal computer.

X-ray Analysis: The structures were solved by direct methods (SIR-97)^[54] and refined by full-matrix least-squares analysis (SHELXL-

97).^[55] All non-hydrogen atoms were refined anisotropically, hydrogen atoms were refined isotropically.

X-ray Crystal Structure of 2: Crystal data at 223 K for C₁₆H₁₁N₃, *M_r* = 245.29, monoclinic, space group *P*2₁/*c*, *D_x* = 1.227 g cm⁻³, *Z* = 8, *a* = 14.8880(5), *b* = 6.9699(3), *c* = 25.5845(11) Å, α = 90.00°, β = 90.539(2)°, γ = 90.00°, *V* = 2654.7(2) Å³. Bruker–Nonius Kappa-CCD diffractometer, Mo-*K α* radiation, λ = 0.7107 Å, μ = 0.075 mm⁻¹. A black crystal of **2** (linear dimensions ca. 0.33 × 0.09 × 0.07 mm) was obtained by slow evaporation of a solution of **2** in CH₂Cl₂ at 25 °C. The numbers of measured and unique reflections are 7433 and 4079, respectively (*R*_{int} = 0.081). Final *R*(*F*) = 0.0609, *wR*(*F*²) = 0.1539 for 431 parameters and 4079 reflections with *I* > 2σ(*I*) and 2.753 < θ < 24.108° (the corresponding *R* values based on all 7433 reflections are 0.0927 and 0.1748, respectively).

X-ray Crystal Structure of 3: Crystal data at 220 K for C₁₈H₁₁N₃, *M_r* = 269.30, triclinic, space group *P*1̄ (no. 2), *D_x* = 1.254 g cm⁻³, *Z* = 2, *a* = 8.9841(12), *b* = 9.0879(12), *c* = 10.2202(13) Å, α = 68.626(18)°, β = 76.636(19)°, γ = 67.430(11)°, *V* = 713.49(16) Å³. Bruker–Nonius Kappa-CCD diffractometer, Mo-*K α* radiation, λ = 0.7107 Å, μ = 0.076 mm⁻¹. A blue crystal of **3** (linear dimensions ca. 0.10 × 0.05 × 0.03 mm) was grown by slow diffusion of hexanes into a CH₂Cl₂ solution of **3** at 25 °C. The numbers of measured and unique reflections are 2993 and 1863, respectively (*R*_{int} = 0.095). Final *R*(*F*) = 0.089, *wR*(*F*²) = 0.196 for 193 parameters and 1005 reflections with *I* > 2σ(*I*) and 5.58 < θ < 22.99° (the corresponding *R* values based on all 1863 reflections are 0.167 and 0.238, respectively).

X-ray Crystal Structure of 12: Crystal data at 223 K for C₁₆H₁₃N₃, *M_r* = 247.30, monoclinic, space group *P*2₁/*c*, *D_x* = 1.199 g cm⁻³, *Z* = 4, *a* = 7.9783(5), *b* = 13.3236(10), *c* = 13.4951(8) Å, α = 90.00°, β = 107.212(4)°, γ = 90.00°, *V* = 1370.3(2) Å³. Bruker–Nonius Kappa-CCD diffractometer, Mo-*K α* radiation, λ = 0.7107 Å, μ = 0.073 mm⁻¹. A dark-brown crystal of **12** (linear dimensions ca. 0.24 × 0.09 × 0.09 mm) was obtained by slow evaporation of a solution of **12** in CDCl₃ at 25 °C. The numbers of measured and unique reflections are 4164 and 2451, respectively (*R*_{int} = 0.044). Final *R*(*F*) = 0.0462, *wR*(*F*²) = 0.1303 for 224 parameters and 2451 reflections with *I* > 2σ(*I*) and 2.425 < θ < 25.350° (the corresponding *R* values based on all 4164 reflections are 0.0688 and 0.1513, respectively).

CCDC-802809 (for **2**), -802810 (for **3**), and -802811 (for **12**) contain the supplementary crystallographic data for this paper. These data can be obtained free of charge from The Cambridge Crystallographic Data Centre via www.ccdc.cam.ac.uk/data_request/cif.

General Method for the “One-Pot” Oxidation/Knoevenagel Condensation: Dess–Martin periodinane (1–3 equiv. of a 15% solution in CH₂Cl₂) was added to a solution of the appropriate propargyl alcohol derivative in CH₂Cl₂. The resulting solution was stirred at 25 °C for the indicated time, filtered through a plug of SiO₂ (CH₂Cl₂), and concentrated in vacuo (without heating) to about 50% of its original volume. Malononitrile (1–3 equiv.) and Al₂O₃ (2–12 equiv.) were added and the solution was stirred at the indicated temperature and time. The solvents were evaporated in vacuo and the residue subjected to FC.

{5-[4-(Dimethylamino)phenyl]-2,4-pentadiyn-1-ylidene}malononitrile (2): The title compound was prepared from **13** (300 mg, 1.51 mmol) and Dess–Martin periodinane (958 mg, 2.26 mmol) in CH₂Cl₂ (50 mL) according to the general method. The mixture was stirred for 1.5 h. Then malononitrile (176 mg, 2.66 mmol) and Al₂O₃ (1.23 g, 12.05 mmol) were added. The mixture was stirred for 1 h

at 50 °C and purified by FC (CH₂Cl₂/heptane, 8:2, then CH₂Cl₂) to afford **2** (173 mg, 47%) as a dark-red solid. *R*_f = 0.2 (SiO₂, heptane/AcOEt, 8:2); m.p. 142–145 °C. ¹H NMR (300 MHz, CDCl₃): δ = 3.06 (s, 6 H), 6.63 (d, *J* = 9.0 Hz, 2 H), 7.00 (s, 1 H), 7.45 (d, *J* = 9.0 Hz, 2 H) ppm. ¹³C NMR (75 MHz, C₂D₂Cl₄): δ = 39.93, 73.37, 93.40, 100.19, 101.53, 105.13, 111.56, 112.66, 135.05, 140.31, 151.72 (11 out of 13) ppm. IR (neat): ν̄ = 3008, 2905, 2353, 2232, 2154, 1591, 1546, 1520, 1446, 1371, 1312, 1260, 1224, 1198, 1166, 1141, 1122, 1061, 942, 864, 815 cm⁻¹. UV/Vis (CH₂Cl₂): λ_{max} (ε) = 234 (20300), 330 (21800), 343 (21300), 512 nm (33300 M⁻¹cm⁻¹). HRMS (EI): calcd. for C₁₆H₁₁N₃ [M]⁺ 245.0953; found 245.0945.

(2E)-5-[4-(Dimethylamino)phenyl]-2-penten-4-yn-1-ol (14): A solution of Red-Al[®] (1.36 mL, 898 mg, 4.44 mmol, 65% in toluene) was added to a solution of **13** (385 mg, 1.93 mmol) in THF (40 mL) at 0 °C. After 1 h, the mixture was warmed to 25 °C and stirred for 3 h. After cooling to 0 °C, AcOEt (30 mL), H₂O (30 mL), and 1 M aq. NaOH (30 mL) were added. The aqueous phase was extracted with Et₂O (2 × 100 mL) and the combined organic phases were washed with sat. aq. NaCl (150 mL) and dried with MgSO₄. The solvents were evaporated in vacuo and the residue purified by FC (heptane/AcOEt, 95:5, then heptane/AcOEt, 9:1, then heptane/AcOEt, 1:1) to afford **14** (203 mg, 52%) as an orange oil. ¹H NMR (300 MHz, CDCl₃): δ = 1.41 (br. s, 1 H), 2.98 (s, 6 H), 4.23–4.25 (m, 2 H), 5.96 (dt, *J* = 15.7, 1.7 Hz, 1 H), 6.27 (dt, *J* = 15.7, 5.5 Hz, 1 H), 6.63 (d, *J* = 9.1 Hz, 2 H), 7.29–7.34 (m, 2 H) ppm. ¹³C NMR (75 MHz, CDCl₃): δ = 40.25, 63.28, 85.23, 91.47, 109.82, 111.36, 111.70, 132.52, 139.56, 149.89 ppm. IR (neat): ν̄ = 3306, 2859, 2358, 2188, 1888, 1601, 1519, 1445, 1359, 1226, 1189, 1170, 1120, 1083, 1035, 985, 946, 814 cm⁻¹. HRMS (ESI): calcd. for C₁₃H₁₆NO⁺ [MH]⁺ 202.1226; found 202.1226.

{(2E)-5-[4-(Dimethylamino)phenyl]-2-penten-4-yn-1-ylidene}malononitrile (12): The title compound was prepared from **14** (185 mg, 0.92 mmol) and Dess–Martin periodinane (585 mg, 1.38 mmol) in CH₂Cl₂ (20 mL) according to the general method. The mixture was stirred for 1 h. Then malononitrile (172 mg, 2.60 mmol) and Al₂O₃ (225 mg, 2.21 mmol) were added. The mixture was stirred for 6 h at 50 °C and purified by FC (CH₂Cl₂/heptane, 8:2) to afford **12** (87 mg, 38%) as a red solid. *R*_f = 0.2 (SiO₂, heptane/AcOEt, 8:2); m.p. 119–121 °C. ¹H NMR (300 MHz, CDCl₃): δ = 3.05 (s, 6 H), 6.59–6.67 (m, 3 H), 6.99 (dd, *J* = 11.8 Hz, 1 H), 7.37–7.45 (m, 3 H) ppm. ¹³C NMR (75 MHz, CDCl₃): δ = 40.10, 81.31, 89.69, 107.38, 110.27, 111.58, 113.70, 130.69, 131.12, 134.23, 151.31, 158.59 (12 out of 13) ppm. IR (neat): ν̄ = 3038, 2918, 2851, 2360, 2221, 2155, 1734, 1606, 1557, 1538, 1444, 1369, 1259, 1222, 1184, 1093, 1066, 1018, 963, 942, 812, 792 cm⁻¹. UV/Vis (CH₂Cl₂): λ_{max} (ε) = 294 (sh, 12000), 321 (14800), 505 nm (35900 M⁻¹cm⁻¹). HRMS (EI): calcd. for C₁₆H₁₃N₃ [M]⁺ 247.1104; found 247.1105.

7-[4-(Dimethylamino)phenyl]-2,4,6-heptatriyn-1-ol (17): A solution of the Hay catalyst in CH₂Cl₂ (2.5 mL) was added to the alkyne **15** (76 mg, 0.45 mmol) and prop-2-yn-1-ol (0.11 mL, 1.91 mmol) in CH₂Cl₂ (30 mL). The resulting mixture was stirred, exposed to air, for 16 h at 25 °C. The solvent was evaporated in vacuo and the residue purified by FC (heptane/AcOEt, 8:2, then heptane/AcOEt, 1:1) to afford **17** (53 mg, 53%) as a light-brown oil. ¹H NMR (300 MHz, CDCl₃): δ = 1.63 (t, *J* = 6.3 Hz, 1 H), 3.0 (s, 6 H), 4.39 (d, *J* = 5.9 Hz, 2 H), 6.59 (d, *J* = 8.7 Hz, 2 H), 7.39 (d, *J* = 9.0 Hz, 2 H) ppm. ¹³C NMR (75 MHz, CDCl₃): δ = 40.08, 51.64, 64.52, 65.33, 71.35, 72.71, 79.50, 106.22, 111.49, 134.37, 150.72 (11 out of 12) ppm. HRMS (EI): calcd. for C₁₅H₁₃NO [M]⁺ 223.0992; found 223.0991.

{7-[4-(Dimethylamino)phenyl]-2,4,6-heptatriyn-1-ylidene}malononitrile (3): The title compound was prepared from **17** (50 mg,

0.22 mmol) and Dess–Martin periodinane (143 mg, 0.34 mmol) in CH₂Cl₂ (40 mL) according to the general method. The mixture was stirred for 1 h. Then malononitrile (18 mg, 0.27 mmol) and Al₂O₃ (74 mg, 0.73 mmol) were added. The mixture was stirred for 1 h at 50 °C and purified by FC (CH₂Cl₂/heptane, 8:2, then CH₂Cl₂) to afford **3** (29 mg, 48%) as a dark-blue metallic solid; m.p. > 180 °C (*caution! explosive decomposition*). ¹H NMR (300 MHz, CDCl₃): δ = 3.05 (s, 6 H), 6.61 (d, *J* = 9.1 Hz, 2 H), 6.97 (s, 1 H), 7.45 (d, *J* = 9.1 Hz, 2 H) ppm. ¹³C NMR (75 MHz, C₂D₂Cl₄): δ = 40.51, 65.91, 72.91, 82.73, 91.07, 96.25, 100.09, 104.79, 111.70, 112.04, 112.76, 120.58, 135.55, 140.47, 151.70 ppm. IR (neat): ν̄ = 3001, 2918, 2229, 2104, 2061, 1598, 1543, 1397, 1372, 1329, 1232, 1184, 1067, 899, 806 cm⁻¹. UV/Vis (CH₂Cl₂): λ_{max} (ε) = 269 (sh, 19400), 276 (21400), 328 (15800), 375 (20500), 538 nm (16100 M⁻¹cm⁻¹). HRMS (EI): calcd. for C₁₈H₁₁N₃ [M]⁺ 269.0948; found 269.0947.

7-[4-(Dihexylamino)phenyl]-2,4,6-heptatriyn-1-ol (18): A solution of the Hay catalyst in CH₂Cl₂ (40 mL) was added to alkyne **16** (413 mg, 1.33 mmol) and prop-2-yn-1-ol (1.18 mL, 20.22 mmol) in CH₂Cl₂/MeOH/THF (1:1:1; 60 mL). The resulting mixture was stirred, exposed to air, for 2 h at 25 °C. The solvent was evaporated in vacuo and the residue purified by FC (heptane then heptane/AcOEt, 8:2, then heptane/AcOEt, 1:1) to afford **18** (330 mg, 68%) as a brown oil. ¹H NMR (300 MHz, CDCl₃): δ = 0.85–0.92 (m, 6 H), 1.24–1.31 (m, 12 H), 1.54–1.64 (m, 5 H), 3.26 (t, *J* = 7.7 Hz, 4 H), 4.39 (d, *J* = 5.5 Hz, 2 H), 6.5 (d, *J* = 9.3 Hz, 2 H), 7.35 (d, *J* = 9.1 Hz, 2 H) ppm. ¹³C NMR (75 MHz, CDCl₃): δ = 13.93, 22.56, 26.64, 27.01, 31.56, 50.83, 51.62, 64.59, 65.28, 71.27, 72.48, 79.78, 104.91, 111.00, 134.59, 148.80 (16 out of 17) ppm. IR (neat): ν̄ = 3366, 2924, 2852, 2361, 2172, 1597, 1517, 1465, 1402, 1363, 1293, 1253, 1186, 1000, 810 cm⁻¹. HRMS (EI): calcd. for C₂₅H₃₃NO [M]⁺ 363.2557; found 363.2556.

{7-[4-(Dihexylamino)phenyl]-2,4,6-heptatriyn-1-ylidene}malononitrile (4): The title compound was prepared from **18** (92 mg, 0.25 mmol) and Dess–Martin periodinane (161 mg, 0.38 mmol) in CH₂Cl₂ (35 mL) according to the general method. The mixture was stirred for 1.5 h. Then malononitrile (25 mg, 0.38 mmol) and Al₂O₃ (116 mg, 1.14 mmol) were added. The mixture was stirred for 1 h at 50 °C and purified by FC (CH₂Cl₂/pentane, 1:1, then CH₂Cl₂) to afford **4** (20 mg, 19%) as a blue metallic solid; m.p. 65–67 °C. ¹H NMR (300 MHz, CDCl₃): δ = 0.9 (t, *J* = 6.5 Hz, 6 H), 1.26–1.32 (m, 12 H), 1.55–1.58 (m, 4 H), 3.29 (t, *J* = 7.8 Hz, 4 H), 6.53 (d, *J* = 9.0 Hz, 2 H), 6.97 (s, 1 H), 7.40 (d, *J* = 9.0 Hz, 2 H) ppm. ¹³C NMR (75 MHz, CDCl₃): δ = 14.12, 22.73, 26.78, 27.2, 31.69, 51.04, 65.48, 72.42, 73.59, 82.50, 90.76, 95.98, 99.87, 103.53, 111.22, 112.29, 135.28, 139.63, 149.62 (19 out of 20) ppm. IR (neat): ν̄ = 2924, 2854, 2340, 2174, 2116, 2074, 1593, 1552, 1520, 1409, 1362, 1294, 1257, 1180, 1016, 812, 795 cm⁻¹. UV/Vis (CH₂Cl₂): λ_{max} (ε) = 278 (17000), 332 (13200), 382 (16000), 560 nm (12700 M⁻¹cm⁻¹). HRMS (FT-MALDI, 3-HPA): calcd. for C₂₈H₃₂N₃ [MH]⁺ 410.2591; found 410.2584. C₂₈H₃₁N₃ (409.57): C 82.11, H 7.63, N 10.26; found C 81.65, H 7.63, N 9.78.

11-[4-(Dihexylamino)phenyl]-2,4,6,8,10-undecapentayn-1-ol (22) and 4,4'-(1,3,5,7,9,11-dodecahexayne-1,12-diyl)bis(*N,N*-dihexylaniline) (23)^[45]

TMS Cleavage of 20: K₂CO₃ (995 mg, 7.20 mmol) was added to a solution of the TMS-protected alkyne **20** (141 mg, 0.93 mmol) in MeOH/THF (1:1; 10 mL). The mixture was stirred for 2 h at 25 °C. CH₂Cl₂ (70 mL) was added and the organic layer was washed with H₂O (70 mL), dried with MgSO₄, and filtered. The resulting solution of deprotected alkyne **20** was concentrated to around 30% of its initial volume in vacuo and used directly in the oxidative coupling step.

TMS Cleavage of 21: K_2CO_3 (86 mg, 0.62 mmol) was added to a solution of the TMS-protected triyne **21** (30 mg, 0.074 mmol) in MeOH/THF (1:1; 6 mL). The resulting mixture was stirred for 2 h at 25 °C. CH_2Cl_2 (40 mL) was added and the organic layer was washed with H_2O (40 mL), dried with MgSO_4 , and filtered. The resulting solution of deprotected triyne **21** was concentrated to around 50% of its initial volume in vacuo and used directly in the next step.

Oxidative Hay Coupling: A solution of the Hay catalyst in CH_2Cl_2 (3 mL) was added to a solution of the deprotected alkyne **21** (25 mg, 0.074 mmol) and deprotected **20** (75 mg, 0.93 mmol) in MeOH/THF/ CH_2Cl_2 (1:1:1; 30 mL) and the resulting mixture was stirred, exposed to air, for 16 h at 25 °C. The mixture was pre-adsorbed on SiO_2 and purified by FC (pentane, then pentane/AcOEt, 8:2, then pentane/AcOEt, 1:1, then AcOEt) to afford **22** (7 mg, 23%) as a red-brown solid and **23** (6 mg, 24%) as an orange solid (yields over two steps).

22: $R_f = 0.2$ (SiO_2 , heptane/AcOEt, 8:2). ^1H NMR (300 MHz, CDCl_3): $\delta = 0.90$ (t, $J = 6.6$ Hz, 6 H), 1.21–1.31 (m, 12 H), 1.56–1.68 (m, 5 H), 3.27 (t, $J = 7.7$ Hz, 4 H), 4.38 (s, 2 H), 6.50 (d, $J = 9.1$ Hz, 2 H), 7.37 (d, $J = 8.8$ Hz, 2 H) ppm. ^{13}C NMR (125 MHz, CDCl_3): $\delta = 14.13, 22.73, 26.80, 27.18, 31.71, 50.99, 51.64, 62.19, 63.67, 63.83, 64.47, 64.53, 67.28, 70.96, 73.19, 80.18, 103.96, 111.11, 135.09, 149.05$ (20 out of 21) ppm. IR (neat): $\tilde{\nu} = 3362, 2955, 2922, 2852, 2360, 2342, 2177, 2087, 1700, 1595, 1519, 1464, 1401, 1364, 1258, 1224, 1187, 1091, 1018, 863, 810$ cm^{-1} . UV/Vis (CH_2Cl_2): λ_{max} (ϵ) = 239 (8700), 256 (9100), 266 (12400), 309 (4000), 328 (4200), 347 (4600), 370 (4600), 384 (sh, 3900), 423 (4700), 456 nm (4000 $\text{M}^{-1}\text{cm}^{-1}$). HRMS (FT-MALDI, 3-HPA): calcd. for $\text{C}_{29}\text{H}_{34}\text{NO}$ $[\text{MH}]^+$ 412.2635; found 412.2635.

23: Analytical data were identical to those reported for **23**.^[45]

{9-[4-(Dihexylamino)phenyl]-2,4,6,8-nonatrayn-1-ylidene}malononitrile (5): The title compound was prepared from **19**^[45] (19 mg, 0.049 mmol) and Dess–Martin periodinane (31 mg, 0.074 mmol) in CH_2Cl_2 (6 mL) according to the general method. The mixture was stirred for 10 min. Then malononitrile (5 mg, 0.079 mmol) and Al_2O_3 (16 mg, 0.159 mmol) were added. The mixture was stirred for 1 h at 25 °C and purified by FC (pentane, then pentane/AcOEt, 95:5, then pentane/AcOEt, 9:1) to afford **5** (8 mg, 38%) as a dark-blue solid. $R_f = 0.5$ (SiO_2 , heptane/AcOEt, 8:2); m.p. > 40 °C (decomp.). ^1H NMR (300 MHz, CDCl_3): $\delta = 0.9$ [t, $^3J(\text{H,H}) = 6.2$ Hz, 6 H], 1.24–1.31 (m, 12 H), 1.55 (br. s, 4 H), 3.29 [t, $^3J(\text{H,H}) = 7.6$ Hz, 4 H], 6.52 [d, $^3J(\text{H,H}) = 9.3$ Hz, 2 H], 6.95 (s, 1 H), 7.40 [d, $^3J(\text{H,H}) = 9.0$ Hz, 2 H] ppm. ^{13}C NMR (75 MHz, CDCl_3): $\delta = 14.04, 22.67, 26.75, 27.16, 29.74, 31.66, 66.84, 70.35, 73.48, 73.56, 81.47, 86.06, 97.55, 98.69, 103.50, 111.01, 111.28, 111.37, 112.15, 135.54, 139.36, 149.72$ ppm. IR (neat): $\tilde{\nu} = 2957, 2921, 2852, 2360, 2342, 2178, 2153, 2069, 1729, 1595, 1554, 1524, 1464, 1425, 1402, 1362, 1293, 1259, 1191, 1096, 1016, 884, 796$ cm^{-1} . UV/Vis (CH_2Cl_2): λ_{max} (ϵ) = 234 (21200), 300 (21800), 362 (17400), 402 (17700), 573 nm (10100 $\text{M}^{-1}\text{cm}^{-1}$). HRMS (FT-MALDI, 3-HPA): calcd. for $\text{C}_{30}\text{H}_{31}\text{N}_3$ $[\text{M}]^+$ 433.2513; found 433.2513.

Supporting Information (see footnote on the first page of this article): UV/Vis spectra, X-ray structure and electrochemistry details.

Acknowledgments

This work was supported by the ETH Research Council and the European Research Council (ERC Advanced Investigators, grant number 246637, “OPTELOMAC”). We also acknowledge partial support from the Pennsylvania Department of Community and

Economic Development through the Ben Franklin Technology Development Authority.

- [1] S. Barlow, S. R. Marder, in: *Functional Organic Materials* (Ed.: T. J. J. Müller, U. H. F. Bunz), Wiley-VCH, Weinheim, Germany, **2007**, pp. 393–437.
- [2] C. Bosshard, R. Spreiter, P. Günter, R. R. Tykwinski, M. Schreiber, F. Diederich, *Adv. Mater.* **1996**, *8*, 231–234.
- [3] a) J. C. May, J. H. Lim, I. Biaggio, N. N. P. Moonen, T. Michinobu, F. Diederich, *Opt. Lett.* **2005**, *30*, 3057–3059; b) N. N. P. Moonen, W. C. Pomerantz, R. Gist, C. Boudon, J.-P. Gisselbrecht, T. Kawai, A. Kishioka, M. Gross, M. Irie, F. Diederich, *Chem. Eur. J.* **2005**, *11*, 3325–3341.
- [4] a) T. Michinobu, J. C. May, J. H. Lim, C. Boudon, J.-P. Gisselbrecht, P. Seiler, M. Gross, I. Biaggio, F. Diederich, *Chem. Commun.* **2005**, 737–739; b) T. Michinobu, C. Boudon, J.-P. Gisselbrecht, P. Seiler, B. Frank, N. N. P. Moonen, M. Gross, F. Diederich, *Chem. Eur. J.* **2006**, *12*, 1889–1905.
- [5] M. Kivala, F. Diederich, *Acc. Chem. Res.* **2009**, *42*, 235–248.
- [6] S.-I. Kato, M. T. R. Beels, P. La Porta, W. B. Schweizer, C. Boudon, J.-P. Gisselbrecht, I. Biaggio, F. Diederich, *Angew. Chem.* **2010**, *122*, 6343–6347; *Angew. Chem. Int. Ed.* **2010**, *49*, 6207–6211.
- [7] B. Esembeson, M. L. Scimeca, T. Michinobu, F. Diederich, I. Biaggio, *Adv. Mater.* **2008**, *20*, 4584–4587.
- [8] J. Leuthold, W. Freude, J.-M. Brosi, R. Baets, P. Dumon, I. Biaggio, M. L. Scimeca, F. Diederich, B. Frank, C. Koos, *Proc. IEEE* **2009**, *97*, 1304–1316.
- [9] C. Koos, P. Vorreau, T. Vallaitis, P. Dumon, W. Bogaerts, R. Baets, B. Esembeson, I. Biaggio, T. Michinobu, W. Freude, J. Leuthold, *Nature Photon.* **2009**, *3*, 216–219.
- [10] J. A. Armstrong, N. Bloembergen, J. Ducuing, P. S. Pershan, *Phys. Rev.* **1962**, *127*, 1918–1939.
- [11] R. R. Tykwinski, U. Gubler, R. E. Martin, F. Diederich, C. Bosshard, P. Günter, *J. Phys. Chem. B* **1998**, *102*, 4451–4465.
- [12] U. Gubler, R. Spreiter, C. Bosshard, P. Günter, R. R. Tykwinski, F. Diederich, *Appl. Phys. Lett.* **1998**, *73*, 2396–2398.
- [13] N. N. P. Moonen, F. Diederich, *Org. Biomol. Chem.* **2004**, *2*, 2263–2266.
- [14] N. N. P. Moonen, R. Gist, C. Boudon, J.-P. Gisselbrecht, P. Seiler, T. Kawai, A. Kishioka, M. Gross, M. Irie, F. Diederich, *Org. Biomol. Chem.* **2003**, *1*, 2032–2034.
- [15] H. Meier, J. Gerold, H. Kolshorn, B. Mühlhling, *Chem. Eur. J.* **2004**, *10*, 360–370.
- [16] N. K. Pahadi, D. H. Camacho, Y. Nakamura, Y. Yamamoto, *J. Org. Chem.* **2006**, *71*, 1152–1155.
- [17] F. Bureš, W. B. Schweizer, J. C. May, C. Boudon, J.-P. Gisselbrecht, M. Gross, I. Biaggio, F. Diederich, *Chem. Eur. J.* **2007**, *13*, 5378–5387.
- [18] J. C. May, I. Biaggio, F. Bureš, F. Diederich, *Appl. Phys. Lett.* **2007**, *90*, 251106-1–251106-3.
- [19] a) M. G. Kuzyk, *Opt. Lett.* **2000**, *25*, 1183–1185; b) A. D. Slepukov, F. R. Hegmann, S. Eisler, E. Elliot, R. R. Tykwinski, *J. Chem. Phys.* **2004**, *120*, 6807–6810.
- [20] T. Gibtnier, F. Hampel, J. P. Gisselbrecht, A. Hirsch, *Chem. Eur. J.* **2002**, *8*, 408–432.
- [21] J. P. Gisselbrecht, N. N. P. Moonen, C. Boudon, M. B. Nielsen, F. Diederich, M. Gross, *Eur. J. Org. Chem.* **2004**, 2959–2972.
- [22] K. Qvortrup, M. T. Jakobsen, J. P. Gisselbrecht, C. Boudon, F. Jensen, S. B. Nielsen, M. B. Nielsen, *J. Mater. Chem.* **2004**, *14*, 1768–1773.
- [23] M. Jain, J. Chandrasekhar, *J. Phys. Chem.* **1993**, *97*, 4044–4049.
- [24] J. Y. Lee, S. B. Suh, K. S. Kim, *J. Chem. Phys.* **2000**, *112*, 344–348.
- [25] R. G. E. Morales, C. Gonzáles-Rojas, *J. Phys. Org. Chem.* **2005**, *18*, 941–944.
- [26] A. Slama-Schwok, M. Blanchard-Desce, J.-M. Lehn, *J. Phys. Chem.* **1990**, *94*, 3894–3902.
- [27] A. Galvan-Gonzalez, G. I. Stegeman, A. K.-Y. Jen, X. Wu, M. Canva, A. C. Kowalczyk, X. Q. Zhang, H. S. Lackritz, S.

- Marder, S. Thayumanavan, G. Levina, *J. Opt. Soc. Am. B* **2001**, *18*, 1846–1853.
- [28] C.-F. Shu, W.-J. Tsai, A. K.-Y. Jen, *Tetrahedron Lett.* **1996**, *37*, 7055–7058.
- [29] S.-J. Kwon, O.-P. Kwon, J.-I. Seo, M. Jazbinsek, L. Mutter, V. Gramlich, Y.-S. Lee, H. Yun, P. Günter, *J. Phys. Chem. C* **2008**, *112*, 7846–7852.
- [30] O.-P. Kwon, S.-J. Kwon, H. Figi, M. Jazbinsek, P. Günter, *Adv. Mater.* **2008**, *20*, 543–545.
- [31] E. M. Graham, V. M. Miskowski, J. W. Perry, D. R. Coulter, A. E. Stiegman, W. P. Schaefer, R. E. Marsh, *J. Am. Chem. Soc.* **1989**, *111*, 8771–8779.
- [32] A. E. Stiegman, E. Graham, K. J. Perry, L. R. Khundkar, L.-T. Cheng, J. W. Perry, *J. Am. Chem. Soc.* **1991**, *113*, 7658–7666.
- [33] C. Dehu, F. Meyers, J. L. Bredas, *J. Am. Chem. Soc.* **1993**, *115*, 6198–6206.
- [34] T. Luu, E. Elliot, A. D. Slepko, S. Eisler, R. McDonald, F. R. Hegmann, R. R. Tykwinski, *Org. Lett.* **2005**, *7*, 51–54.
- [35] S. Eisler, A. D. Slepko, E. Elliot, T. Luu, R. McDonald, F. R. Hegmann, R. R. Tykwinski, *J. Am. Chem. Soc.* **2005**, *127*, 2666–2676.
- [36] V. Alain, L. Thouin, M. Blanchard-Desce, U. Gubler, C. Bosshard, P. Günter, J. Müller, A. Fort, M. Barzoukas, *Adv. Mater.* **1999**, *11*, 1210–1214.
- [37] B. G. Tiemann, L.-T. Cheng, S. R. Marder, *J. Chem. Soc., Chem. Commun.* **1993**, 735–737.
- [38] H. Ikeda, Y. Kawabe, T. Sakai, K. Kawasaki, *Chem. Lett.* **1989**, 1285–1288.
- [39] U. Gubler, Ph. D. Dissertation, ETH No. 13605, ETH Zürich, Switzerland, **2000**.
- [40] M. Blanchard-Desce, V. Alain, P. V. Bedworth, S. R. Marder, A. M. Fort, C. Runser, M. Barzoukas, S. Lebus, R. Wortmann, *Chem. Eur. J.* **1997**, *3*, 1091–1104.
- [41] P. D. Jarowski, M. D. Wodrich, C. S. Wannere, P. v. R. Schleyer, K. N. Houk, *J. Am. Chem. Soc.* **2004**, *126*, 15036–15037.
- [42] S. C. Shim, M. C. Suh, S. C. Suh, X.-L. Huang, E. K. Suh, *Polymer* **2000**, 467–472.
- [43] S. Hatakeyama, M. Yoshida, T. Esumi, Y. Iwabuchi, H. Irie, T. Kawamoto, H. Yamada, M. Nishizawa, *Tetrahedron Lett.* **1997**, *38*, 7887–7890.
- [44] M. Kivala, C. Boudon, J.-P. Gisselbrecht, P. Seiler, M. Gross, F. Diederich, *Angew. Chem.* **2007**, *119*, 6473–6477; *Angew. Chem. Int. Ed.* **2007**, *46*, 6357–6360.
- [45] B. B. Frank, M. Kivala, B. Camafort Blanco, B. Breiten, W. B. Schweizer, P. R. Laporta, I. Biaggio, E. Jahnke, R. R. Tykwinski, C. Boudon, J. P. Gisselbrecht, F. Diederich, *Eur. J. Org. Chem.* **2010**, 2487–2503.
- [46] S. M. E. Simpkins, M. D. Weller, L. R. Cox, *Chem. Commun.* **2007**, 4035–4037.
- [47] A. Kiehl, A. Eberhardt, M. Adam, V. Enkelmann, K. Müllen, *Angew. Chem.* **1992**, *104*, 1623–1626; *Angew. Chem. Int. Ed. Engl.* **1992**, *31*, 1588–1591.
- [48] K. Staub, G. L. Levina, S. Barlow, T. C. Kowalczyk, H. S. Lackritz, M. Barzoukas, A. Fort, S. R. Marder, *J. Mater. Chem.* **2003**, *13*, 825–833.
- [49] J. Zhou, M. G. Kuzyk, *J. Phys. Chem. C* **2008**, *112*, 7978–7982.
- [50] M. J. Frisch, G. W. Trucks, H. B. Schlegel, G. E. Scuseria, M. A. Robb, J. R. Cheeseman, J. Montgomery Jr., T. Vreven, K. N. Kudin, J. C. Burant, J. M. Millam, S. S. Iyengar, J. Tomasi, V. Barone, B. Mennucci, M. Cossi, G. Scalmani, N. Rega, G. A. Petersson, H. Nakatsuji, M. Hada, M. Ehara, K. Toyota, R. Fukuda, J. Hasegawa, M. Ishida, T. Nakajima, Y. Honda, O. Kitao, H. Nakai, M. Klene, X. Li, J. E. Knox, H. P. Hratchian, J. B. Cross, C. Adamo, V. Bakken, C. Adamo, J. Jaramillo, R. Gomperts, R. E. Stratmann, O. Yazyev, A. J. Austin, R. Cammi, C. Pomelli, J. W. Ochterski, P. Y. Ayala, K. Morokuma, G. A. Voth, P. Salvador, J. J. Dannenberg, V. G. Zakrzewski, S. Dapprich, A. D. Daniels, M. C. Strain, O. Farkas, D. K. Malick, A. D. Rabuck, K. Raghavachari, J. B. Foresman, J. V. Ortiz, Q. Cui, A. G. Baboul, S. Clifford, J. Cioslowski, B. B. Stefanov, G. Liu, A. Liashenko, P. Piskorz, I. Komaromi, R. L. Martin, D. J. Fox, T. Keith, M. A. Al-Laham, C. Y. Peng, A. Nanayakkara, M. Challacombe, P. M. W. Gill, B. Johnson, W. Chen, M. W. Wong, C. Gonzalez, J. A. Pople, *Gaussian 03*, rev. C.02, Gaussian, Inc., Wallingford, CT, **2004**.
- [51] F. Furche, K. Burke, *Ann. Rep. Comput. Chem.* **2005**, *1*, 19–30.
- [52] a) D. J. Tozer, *J. Chem. Phys.* **2003**, *119*, 12697–12699; b) A. Dreuw, M. Head-Gordon, *J. Am. Chem. Soc.* **2004**, *126*, 4007–4016.
- [53] M. R. Silva-Junior, M. Schreiber, S. P. A. Sauer, W. Thiel, *J. Chem. Phys.* **2008**, *129*, 104103–104111.
- [54] A. Altomare, M. C. Burla, M. Camalli, G. L. Casciaro, C. Giacovazzo, A. Guagliardi, A. G. G. Moliterni, G. Polidori, R. Spagna, *J. Appl. Crystallogr.* **1999**, *32*, 115–119.
- [55] G. M. Sheldrick, *Acta Crystallogr., Sect. A* **2008**, *64*, 112–122.

Received: March 18, 2011
Published Online: June 7, 2011